Dynamic Orbit Determination of Low Earth Orbit CubeSat

Danlei Chen
Advisor: Dr. S. Asokanthan

Sept 2018 – May 2019

Western Engineering

Contents

Introduction

Canadian CubeSat Project

- Engage selected Canadian university teams to design, build, test, launch their 2U nanosatellite, limited to 3.6kg total mass [1]
- Collaboration of Western University – Nunavut Arctic College CubeSat Project
- 360° Virtual Reality imaging system with Canadensys industry partner for space exploration, Earth observation, outreach

Objective and Scope

- Determine orbit paramters of the CubeSat deployed from LEO and evaluate orbit perturbation factors for the decay of the orbit
- Ensure accurate prediction for the predicted orbit and lifecycle of the satellite
- Inform mission preparation, operational cycle, and post-operational analysis
- Perform concurrent design with interdisciplinary engineering teams, industry

Theoretical Analysis and Literature Review

CubeSats

- First developed in 1999 by California Polytechnic State University and Stanford University [2]
- Low-cost science, education, technology and communications missions for universities, government, private industry [2]
- Ideal for testing new technologies such as modular spacecraft systems, formation flying, launching compact payloads in constellations [3]

CSA Operational Requirements

From CSA Design Specification Document [2]:

- Designed to have an in-orbit lifetime of at least 3 months
- From historical data, some CubeSats can survive up to 2 years dependent on solar activity

Newton’s Laws

- Under ideal conditions, the motion of a satellite in orbit is determined by the gravitational effect between the satellite orbiting body and the primary body [4]
- For a fixed mass system, Newton’s second law describes that the force applied is equal to acceleration of the object with a constant mass [4]

$$\vec{F} = \frac{d m\vec{v}}{dt} \qquad \vec{F} = m\vec{a}$$

Equation 1: Newton’s Newton’s Second Law [4]

Newton's Laws

- Combined with two-body problems considering gravity exerted by a central body, Newton's Law of Gravitation supplies the components of the force of gravity of the Earth on the satellite [4]

- Assumes the mass of the satellite is negligible compared to the central body, coordinate system with respect to an inertial frame [4]

$$\vec{f}_{gravity} = -\frac{G m_{\oplus} m_{sat}}{r^2} \frac{\vec{r}}{|\vec{r}|}$$

$$\ddot{\vec{r}} = -\frac{G(m_{\oplus} + m_{sat})}{r^2} \frac{\vec{r}}{|\vec{r}|}$$

Equation 2: Newton's Law of Gravitation [4]
Equation 3: Two Body Acceleration Equation [4]

Orbital Mechanics

Using orbital mechanics principles, Kepler's first law shows that satellite trajectories follow conic section ellipses. [3]

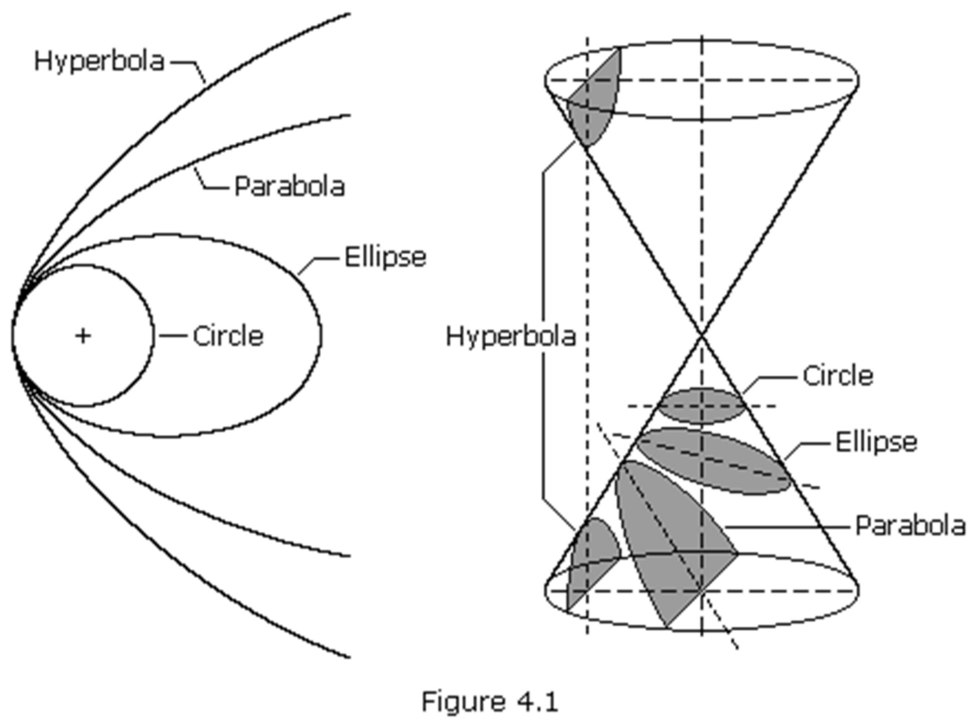

Figure 1:
Conic Section
Ellipse Trajectory [4]

Orbital Perturbation Factors

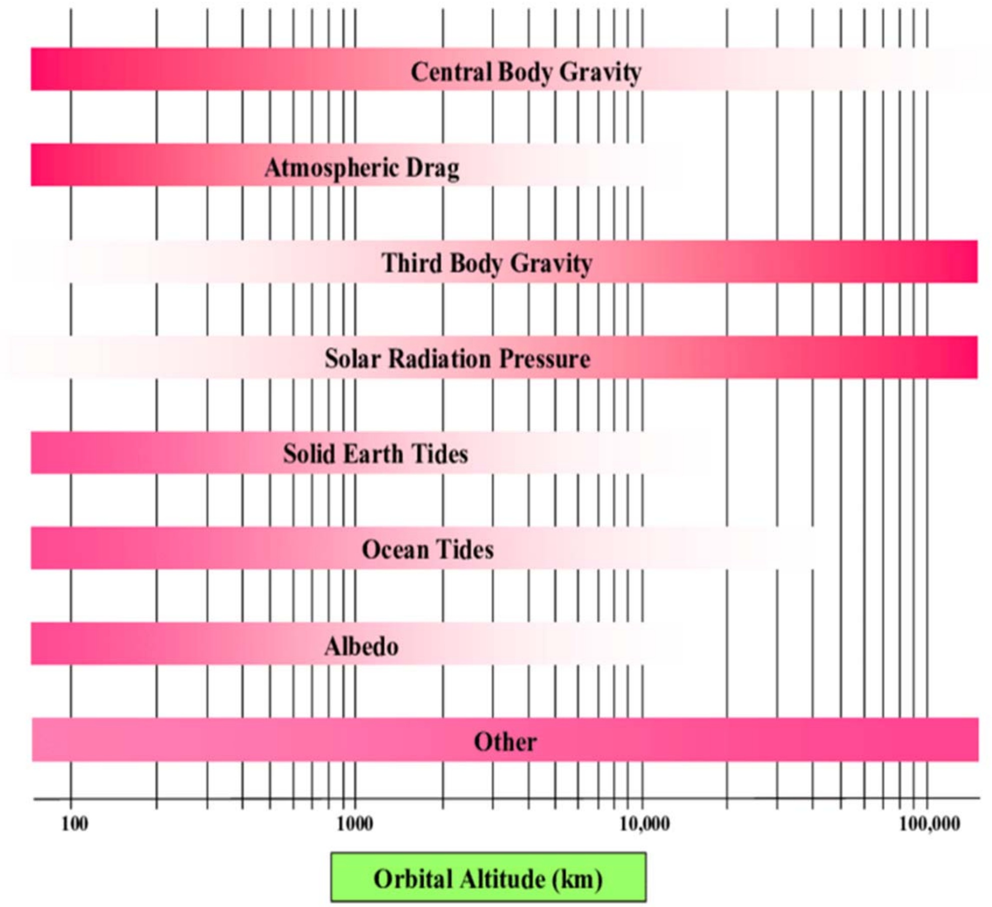

Figure 2: Applicability of Perturbation Effects [4]

Keplerian Acceleration on Satellite

Equation 4: Keplerian Acceleration on Satellite [5]

$$\mathbf{a}_K = -\frac{\mu}{r^3}\mathbf{r}$$

where μ is the Earth's gravitational constant, and r is the spacecraft position vector in the inertial frame

J2 Acceleration on Satellite

Equation 5: J2 Acceleration on Satellite [5]

$$a_{J2} = -\frac{3J_2\mu R_E}{2r^5}\left(1-\frac{5r_z^{\,2}}{r^2}\right)\left(r_x\hat{i}+r_y\hat{j}\right)-\frac{3J_2\mu R_E}{2r^5}\left(3-\frac{5r_z^{\,2}}{r^2}\right)r_z\hat{k},$$

where the J2 is the zone coefficient of Earth’s oblateness, RE is the average radius of the Earth, rx, ry, rz are the spacecraft position vector within the inertial frame in directions i, j, k

Atmospheric Drag Acceleration on Satellite

Equation 7: Atmosphere Drag Acceleration [5]

$$\boldsymbol{a}_D = -\frac{1}{2C_B}\rho V^2 \hat{\boldsymbol{V}},$$

where ρ is the atmospheric density, CB is the ballistic coefficient given by the mass of the satellite divided by the drag area, and V is the velocity

Total Acceleration on Satellite

Equation 6: Total Acceleration on Satellite [5]

$$V_{J2} = \sqrt{a_T \cdot r},$$

The total velocity VJ2 required for maintaining a circular orbit r about the equator with J2 effects, where aT the total acceleration

Two-Line Mean Element Set

- Data format encoding list of orbital elements at the stated epoch time [6]
- Specific to the simplified perturbation model algorithms (NORAD SGP, SGP4, SDP4, SGP8 and SDP8) [6]
  - Orbital state vectors of satellite relative to Earth-centered inertial coordinate system

Two-Line Mean Element Set

- ISS Satellite TLE [6] taken at 2018/309/.55834577 2018/11/05 13:24:01 UTC

```
ISS
1 25544U 98067A   18309.55834577  .00016717  00000-0  10270-3 0  9002
2 25544  51.6428  34.2302 0004382  13.7100 346.4171 15.53914070 20497
```

Orbital Parameters

For the semi-major axis, a:

$$
\begin{aligned}
a &= \frac{\mu^{\frac{1}{3}}}{\frac{2n\pi}{86400}^{\frac{2}{3}}} = \frac{(3.986004418 \times 10^{14})^{\frac{1}{3}}}{\frac{(2)(15.53914070)(\pi)}{86400}^{\frac{2}{3}}} = 6783448.132168m = 6.7834 \times 10^{6} m = \\
a &= 6783.448km
\end{aligned}
$$

where Earth's standard gravitational parameter $\mu = 3.986004418 \times 10^{14} m^3 s^{-2}$
Mean Motion n = 15.53914070 rev/day

Orbital Parameters

For the altitude at perigee:

$$
\begin{aligned}
hp &= a(1-e) - E_r = (6783448.132168)(1-0.0004382) - 6.371 \times 10^6 = 409475.6252m \\
hp &= 409.48km
\end{aligned}
$$

where Semi-major axis a $= 6783448.132168m$
Eccentricity e $= 0.0004382°$
Earth mean radius $\mathrm{E}_r = 6.371 \times 10^6 m$

For the altitude at apogee:

$$
\begin{aligned}
ha &= a(1+e) - E_r = (6783448.132168)(1-0.0004382) - 6.371 \times 10^6 = 415420.6391m \\
ha &= 415.421km
\end{aligned}
$$

where Semi-major axis a $= 6783448.132168m$
Eccentricity e $= 0.0004382°$
Earth mean radius $\mathrm{E}_r = 6.371 \times 10^6 m$

Orbital Parameters

For the orbital period, according to Kepler's Third Law of a small body orbiting the central body in an elliptical orbit:

$$
\begin{aligned}
T &= 2\pi\sqrt{\frac{a^3}{\mu}} = 2\pi\sqrt{\frac{6783448.132168^3}{3.986004418 \times 10^{14}}} = \\
T &= 5560.153014s
\end{aligned}
$$

where Semi-major axis a = $6783448.132168m$
Earth's standard gravitational parameter $\mu = 3.986004418 \times 10^{14} m^3 s^{-2}$

$$
\begin{aligned}
N_{orbits} &= \frac{86400}{T} = \\
N_{orbits} &= 15.107 orbits/day
\end{aligned}
$$

where Orbital period T = 5560.153014s

Orbital Parameters

- Inclination: 51.6428°
- Eccentricity: 0.0004382°
- Argument of perigee: 13.7100 °
- Right ascension of the ascending node (RAAN): 34.2302°
- Mean anomaly: 346.4171°

Methodology of Solution and Numerical Modeling Design

Western Engineering

Orbital Perturbations Methodology

- STK High-Precision Orbit Propagator (HPOP) and STK Lifetime Tool for 110 km deorbit altitude
- Orbit epoch: 1 January 2021 16:00:00.000UTC
- Coordinate Type and System: Classical Coordinate Type, ICRF inertial frame
- Coordinate type based on ISS TLE for launch

Atmospheric Drag Force Models

- Secondary source of perturbations after J2 factor

Equation 8: Acceleration due to Drag Force [10]

$$a_{drag} = \frac{1}{2}\rho V^2 C_D \frac{S}{m}$$

where ρ is the density of the atmosphere, V is the velocity of the body relative to the atmosphere, CD is the coefficient of drag, S is the surface area, and m is the mass of the body

- High uncertainties relating to the density, drag coefficient, velocity of the body wrt the atmosphere

Atmospheric Drag Models

- Significant atmosphere density variations caused by atmospheric heating radiative energy absorbed from extreme ultraviolet (EUV) solar radiation [11]
  - As solar EUV and thermospheric temperature increased by 2x, the thermospheric density increased more than 10x times from solar min to max at 400km [11]
- Upper density varies by energetic events: solar flare events, solar winds, coronal mass ejections, corotating interaction regions, geomagnetic storms, solar magnetic activity cycle [12]

Atmospheric Drag Models

- Geomagnetic perturbations caused by interactions with the Earth's magnetosphere deteriorate the orbit cycle of the satellite and produce greater temperature gradients [12]
- HSSs and CIRs produce storm induced atmospheric disturbance towards the tail of the 11 year trend of the solar magnetic activity cycle [12]
- CME geomagnetic storms result in higher peaks but less total changes in thermosphere density perturbations and orbit decay [13]

Thermospheric Mass Density Empirical Models

- NRL Mass Spectrometer – Incoherent Scatter Extended model (NRLMSISE-00)
- Jacchia models (J64, J70, J71, J77)
- Drag Temperature (DTM) models (DTM2012)
- Harris-Priester
- 1976 Standard
- CIRA 197
- Mars GRAM

Jacchia Atmospheric Density Models

- Typically used for orbital development, parameterized by the temperature at 90km, and mixing ratio of distinct component densities at 90km to 105km
  - Based on observed satellite ephemeris decay density data

Jacchia Atmospheric Density Models

Equation 9: Homosphere Barometric Equation from Earth's surface to 90km above the surface [15]

$$\frac{d\rho}{\rho} = \frac{T}{\bar{M}} d\left(\frac{\bar{M}}{T}\right) - \frac{\bar{M}g}{RT} dz$$

where ρ is the density of the atmosphere, T is the temperature, M is the mean molecular mass, R is the universal gas constant (8.3145 J/mol), z is the altitude, and g is where ga=9.80665ms-2 and Ra = 356.766km.

Jacchia Atmospheric Density Models

Equation 10: Atmospheric Density Equation [15]

$$\rho = \bar{M}N/A$$

where the N=∑ni is the number density, A is Avogadro's number (6.0221409E23) , and the mean molecular mass is: $\bar{M} = \sum_i n_i M_i / N$

Equation 11: Mean Molecular Mass Equation [15]

where ni is the number density of i, Mi is the molecular mass of i, and N=∑ni is the number density.

Jacchia Atmospheric Density Models

- At the upper atmosphere, above 90km from Earth's surface, the atmospheric components (ie: N2, O2, O) act individually

Equation 12: Heterosphere Diffusion Equation [15]

$$\frac{dn_i}{n_i} = -(1 + \alpha_i)\frac{dT}{T} - \frac{M_i g}{RT} dz$$

where ni is the number density of i, Mi is the molecular mass of i, and αi is the coefficient of thermal diffusion of i.

Comparative Testing

- Minor improvements with the NRLMSISE-00 class model based on incoherent scatter radars from Earth and satellite in-situ composition data [14]
- No evidence was found to demonstrate that any single model is better than the others
- For the purposes of this study, the 1977 Jacchia-Roberts and the NRLMISE-2000 models were utilized for the CubeSat orbit determination

Coefficient of Drag and Area/Mass Ratio

- Between 2.0 and 2.2, and is set at CD=2.2 for the entirety of the orbital analysis [17]
- Varies as a function of the satellite shape/orientation and collisions with atmospheric air particles, changes in atmospheric temperature and composition [17]
- Empirical atmospheric density models integrate any drag coefficient errors as density biases [17]

Gravity Force Models

- Earth Gravitational Models (EGM) applied based on Earth's solid-body mass distribution, as a function of a spherical harmonic model [18]
  - Early spherical models harmonic expressions of degree 8 have evolved to current models of degree 2190, such as the EGM2008 model
- Newer progresses in long wavelength gravity force models have determined a more precise EGM with a ±15cm global RMS geoid undulation uncertainty [18]

Gravity Force Models

- EGM2008 model, as an evolution of EGM96, uses a least squares combination and error covariance matrix of the ITG-GRACE03S gravity force model [19]

Equation 13: Geopotential Field V in spherical harmonics to degree N at point (r, Φ, λ) [19]

$$V(r,\phi,\lambda) = \frac{GM}{r}\sum_{n=0}^{N}\left(\frac{a_e}{r}\right)^n \sum_{m=0}^{n}\left[\bar{C}_{nm} cos(m\lambda) + \bar{S}_{nm} sin(m\lambda)\right]\bar{P}_{nm}(\sin\phi)$$

Where, $\bar{C}nm$ and $\bar{S}nm$ are the normalized geopotential coefficients and $\bar{P}nm$ are the normalized Legendre functions, and Sn0= 0.

Gravity Force Models

- Area-mean free-air gravity anomalies as a 300 arcsecond equiangular grid: combination of ground, altimetry, and aerial gravitational observations [18]

- Additional topographical spectral data included in locations of low-resolution gravity data [18]

Gravity Force Models

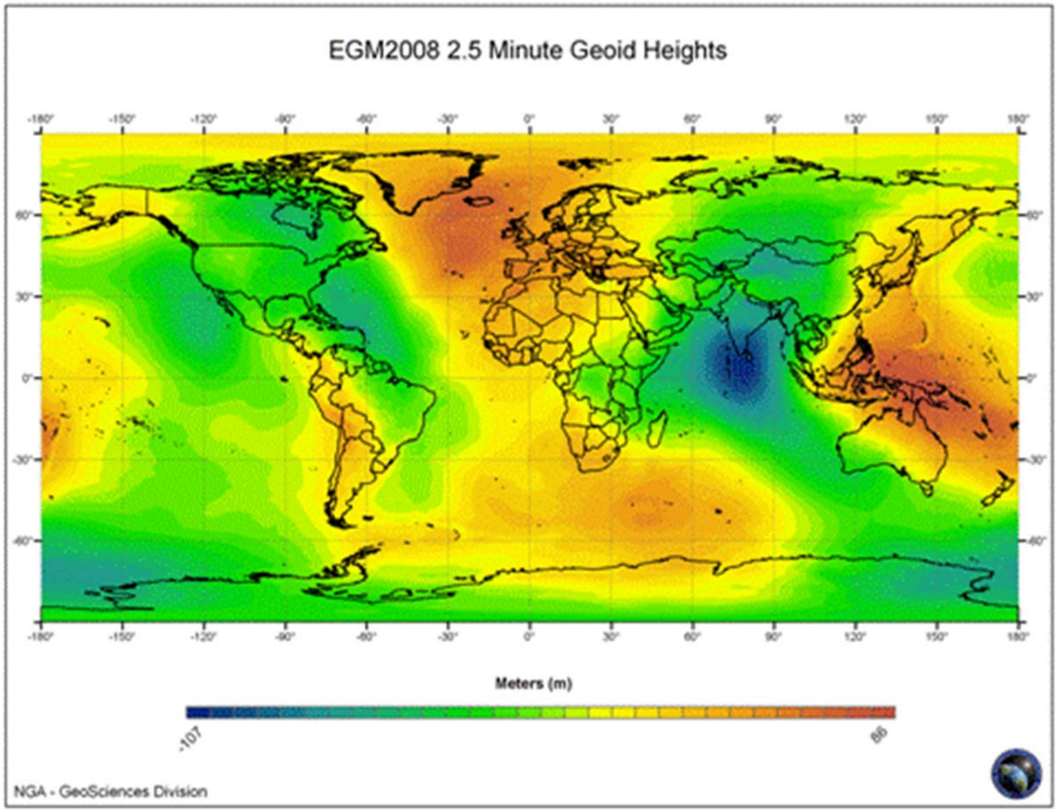

Source: National Geospatial-Intelligence Agency (2008)

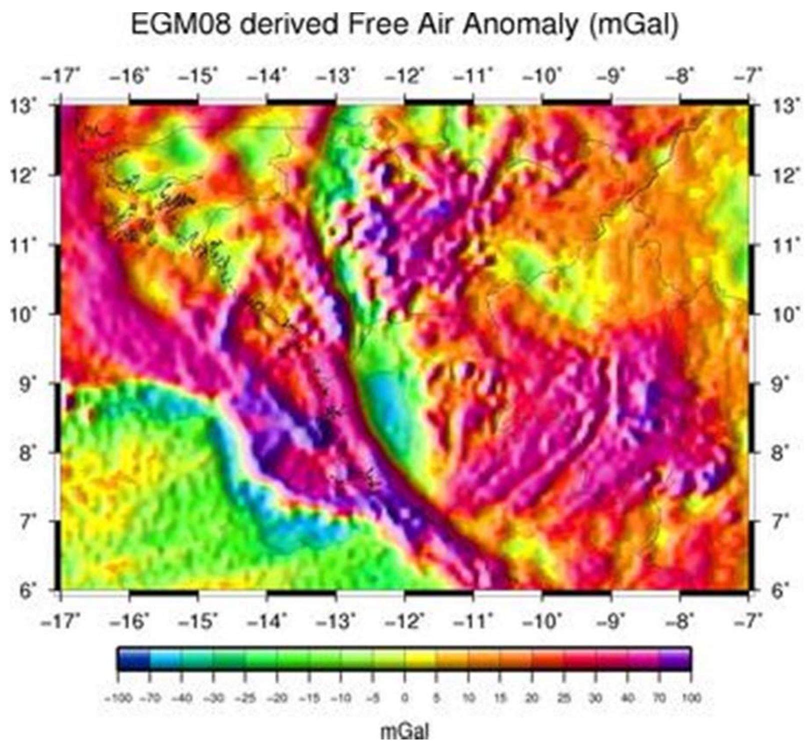

Solar Radiation Pressure Model

- In LEO, the solar radiation pressure (SRP) is negligible, and assumed as the value of 0.9 [20]
- For higher altitudes, SRP as solar photon drag impact upon the satellite is more significant, while atmospheric drag is considered negligible [20]
- SRP is primarily considered as the non-conservative force in geostationary orbits [20]

Uncertainty

- Initial state error covariance matrix: position and velocity uncertainties of the satellite during its simulated orbit [9]
- Two-body force and amplitude oscillation in eccentric orbits effects are more pronounced at the perigee with the highest velocity, decreased at the apogee with the lowest velocity [9]
- Consider analysis: Noise in the model's filters or uncertainties in the parameter values [9]

Results and Discussions

Simulated Orbit Track

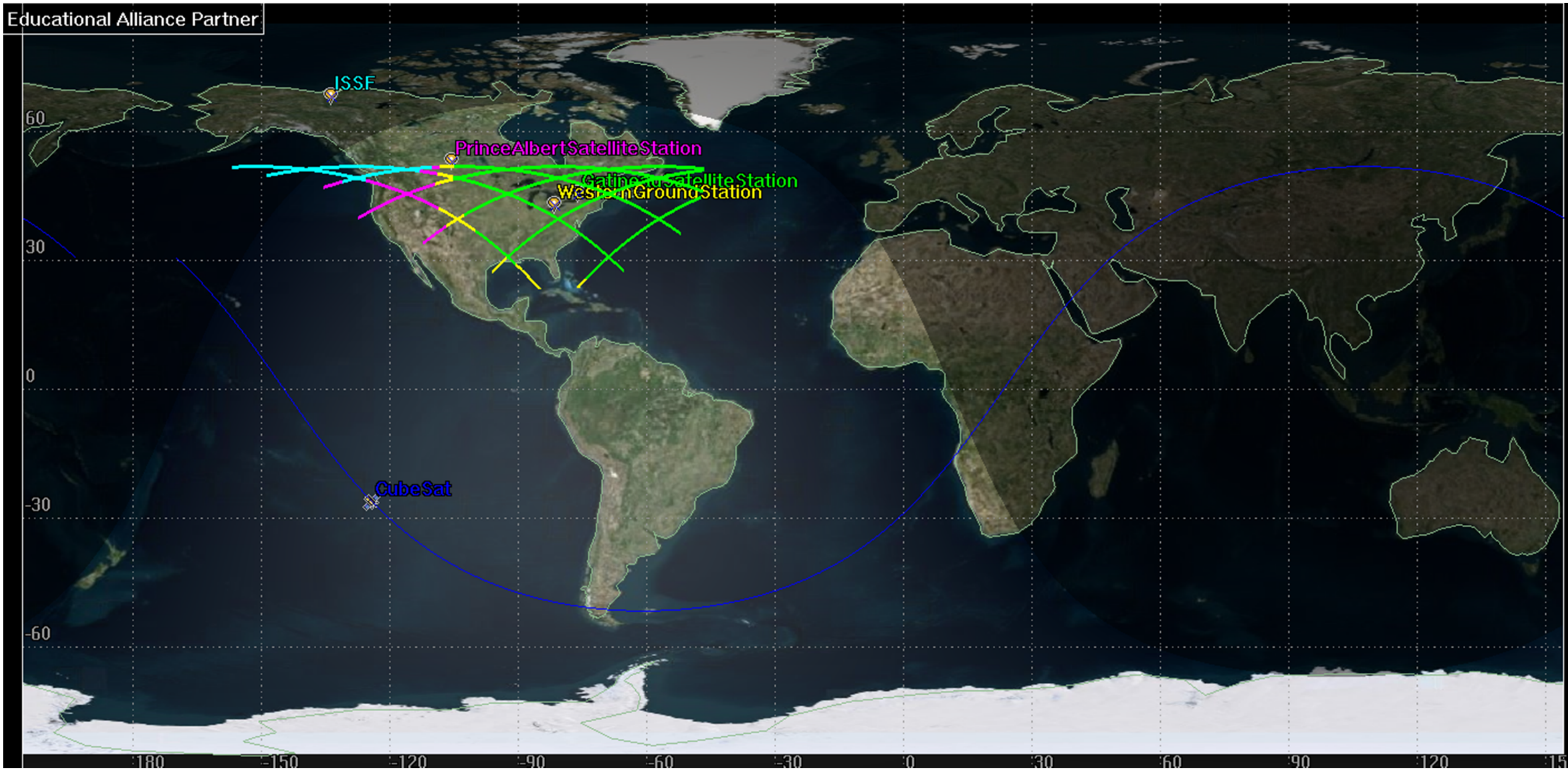

Western Ground Station Access

Place-WesternGroundStation-To-Satellite-CubeSat: Access Summary Report

WesternGroundStation-To-CubeSat

Access	Start Time (UTCG)	Stop Time (UTCG)	Duration (sec)
1	2 Jan 2021 04:39:54.993	2 Jan 2021 04:49:54.917	599.925
2	2 Jan 2021 06:15:55.195	2 Jan 2021 06:26:26.725	631.530
3	2 Jan 2021 07:53:16.903	2 Jan 2021 08:03:03.494	586.590
4	2 Jan 2021 09:30:24.038	2 Jan 2021 09:40:22.972	598.935
5	2 Jan 2021 11:06:51.919	2 Jan 2021 11:17:30.513	638.593
6	2 Jan 2021 12:43:40.885	2 Jan 2021 12:52:42.345	541.460

Global Statistics

	Access	Start Time (UTCG)	Stop Time (UTCG)	Duration (sec)
Min Duration	6	2 Jan 2021 12:43:40.885	2 Jan 2021 12:52:42.345	541.460
Max Duration	5	2 Jan 2021 11:06:51.919	2 Jan 2021 11:17:30.513	638.593
Mean Duration				599.505
Total Duration				3597.033

Worst-Case Scenario

- Drag area and the area exposed to the sun were set for the lateral side of the CubeSat as 0.026786m2 (W×H) for the largest surface
- Mass set to the maximum, 3.6kg allowed by Nanoracks [8]
- Atmospheric density model selected as Jacchia-Roberts 1977 model
- Constant coefficient of drag C_D of 2.2 and coefficient of radiation pressure C_R as 0.9

Worst-Case Scenario HPOP Parameters

- Gravitational Force Model: EGM2008.grv for a maximum degree and order of 21

- Low altitude density model as the NRLMSISE-00, at a blending range of 90km due to the Jacchia-Roberts model covering density computation above 90km

Worst-Case Scenario

Time (UTCG)	Semi-parameter (km)	Semi-major Axis (km)	Eccentricity	Inclination (deg)	Arg of Perigee (deg)	RAAN (deg)	Height of Apogee (km)	Height of Perigee (km)	Sidereal Period (sec)	Orbit Count
42:50.1	6777.471	6777.472	0.000435	51.55812	166.8761	34.41948	402.283	396.3867	5552.807	0
06:20.8	6777.436	6777.437	0.000395	51.55816	172.4934	31.19385	401.9783	396.6227	5552.765	10
23:21.2	6511.864	6511.864	0.000271	51.4885	263.8408	333.9724	135.4884	131.9656	5229.606	8971
50:09.6	6496.525	6496.525	0.000133	51.48648	280.3248	333.6223	119.2511	117.5254	5211.139	8972

Worst-Case Scenario

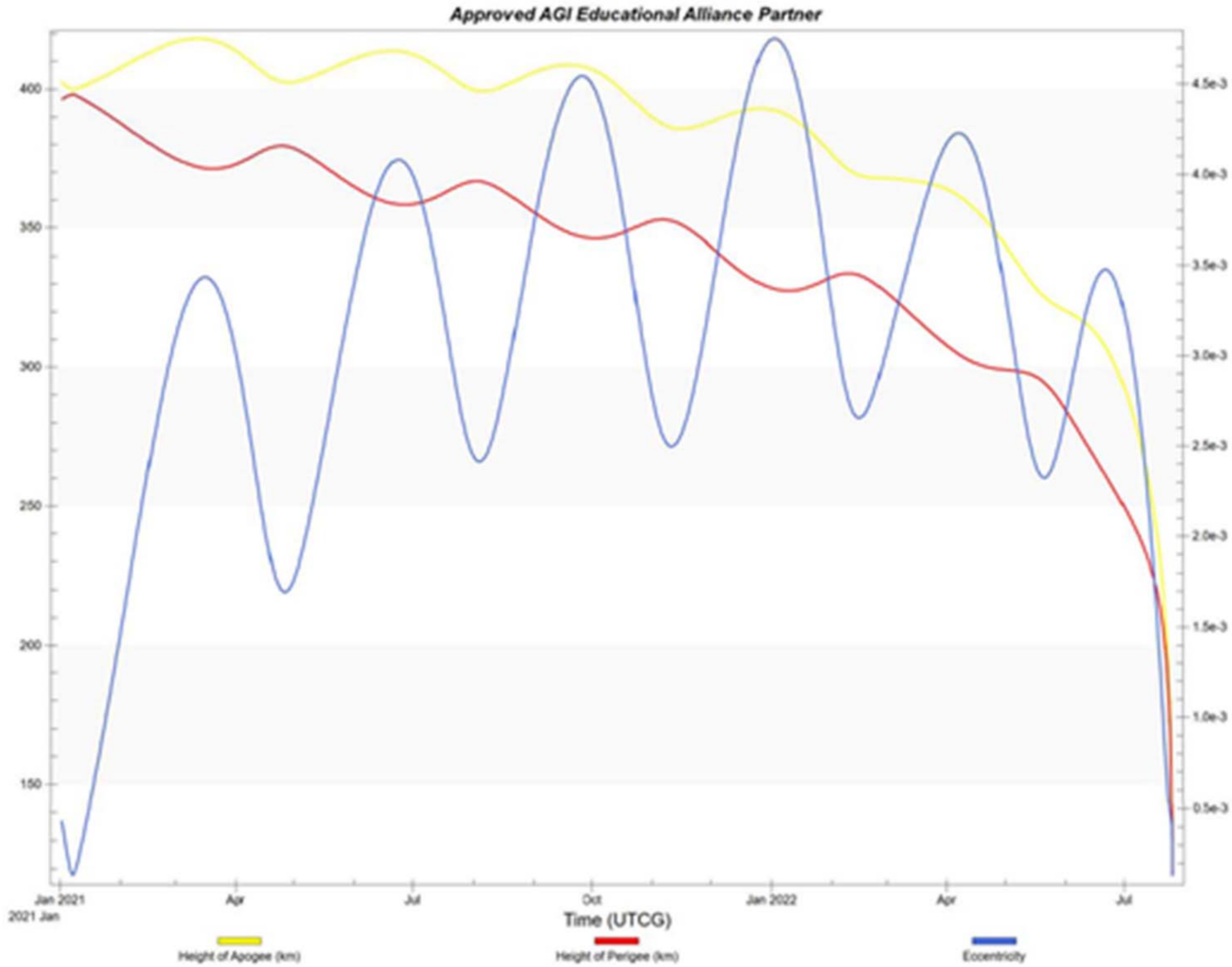

Figure 4: Worst-Case Apogee and Perigee Altitude and Eccentricity [7]

Worst-Case Scenario

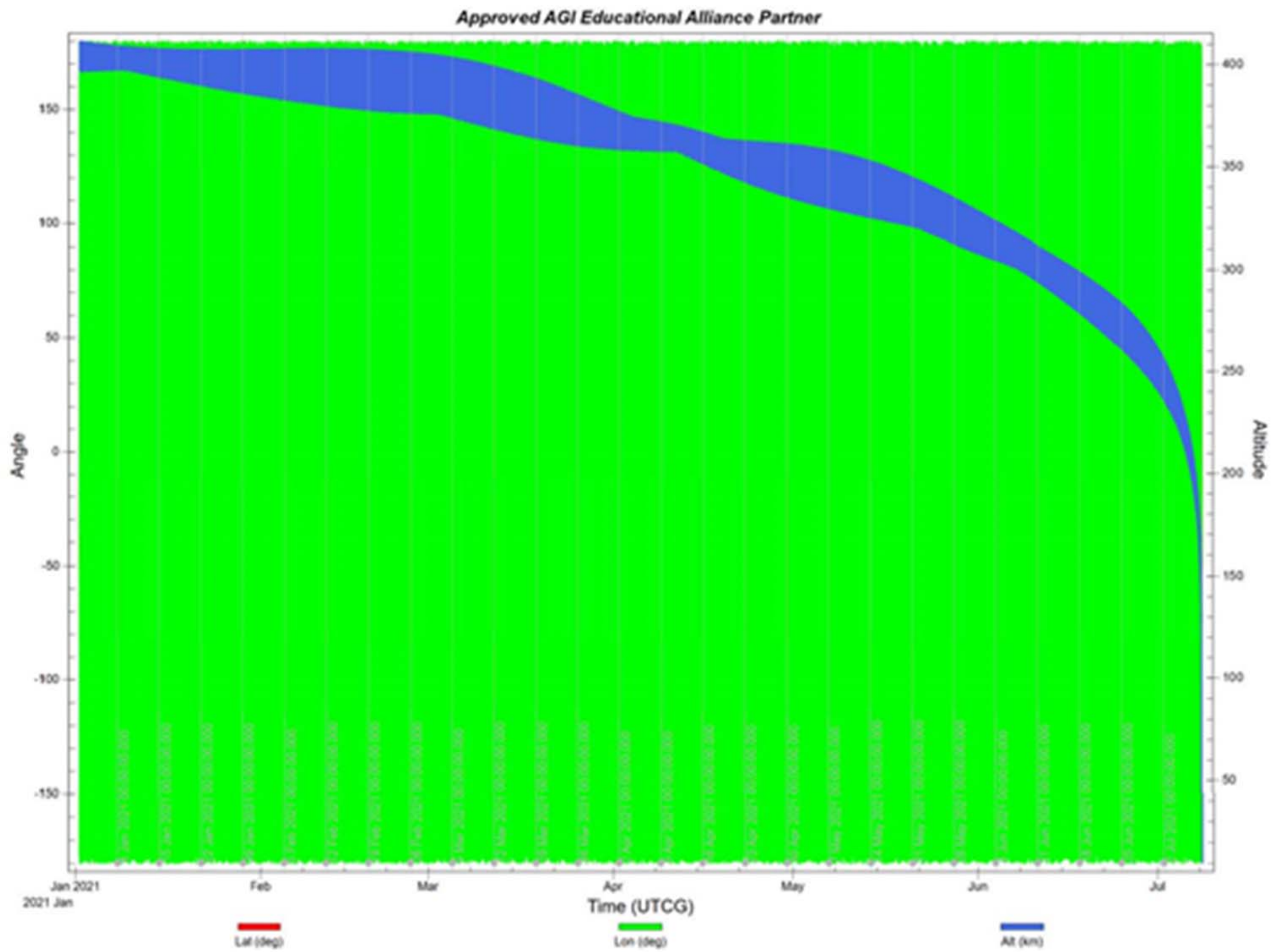

Figure 5: Worst-Case Longitude, Latitude Altitude of CubeSat [7]

Worst-Case Scenario

- Lifetime period with orbit deterioration effects:
  - 8972 orbits
  - 1.6 years
  - January 1 2021 at 16:00:00.000UTC - July 25 2022 at 13:50:09:551
  - Apogee altitude: 119.251142km at de-orbit
  - Perigee altitude: 117.52536km at de-orbit

Best-Case Scenario

- Drag area and the area exposed to the sun were set for the lateral side of the CubeSat as 0.013924m2 (W×L) for the smallest surface
- Mass set to 3.6kg per Nanoracks [8]
- Atmospheric density model selected as NRLMSISE-00 model
- Constant coefficient of drag C_D of 2.2 and coefficient of radiation pressure C_R as 0.9

Best-Case Scenario HPOP Parameters

- Gravitational Force Model: EGM2008.grv for a maximum degree and order of 21
- Low altitude density model as the NRLMSISE-00, as it provided considerations for the lower Earth atmospheric model

Best-Case Scenario

Time (UTCG)	Semi-parameter (km)	Semi-major Axis (km)	Eccentricity	Inclination (deg)	Arg of Perigee (deg)	RAAN (deg)	Height of Apogee (km)	Height of Perigee (km)	Sidereal Period (sec)	Orbit Count
42:50.1	6777.471	6777.472	0.000435	51.55812	166.8761	34.41948	402.283	396.3867	5552.807	0
06:21.0	6777.455	6777.456	0.000395	51.55816	172.5725	31.19385	401.9957	396.6426	5552.788	10
55:37.9	6505.743	6505.743	0.000346	51.48581	57.16249	353.6301	129.8549	125.3579	5222.235	14450
22:22.3	6496.058	6496.058	0.00016	51.48456	57.90607	353.2795	118.9592	116.8827	5210.577	14451

Best-Case Scenario

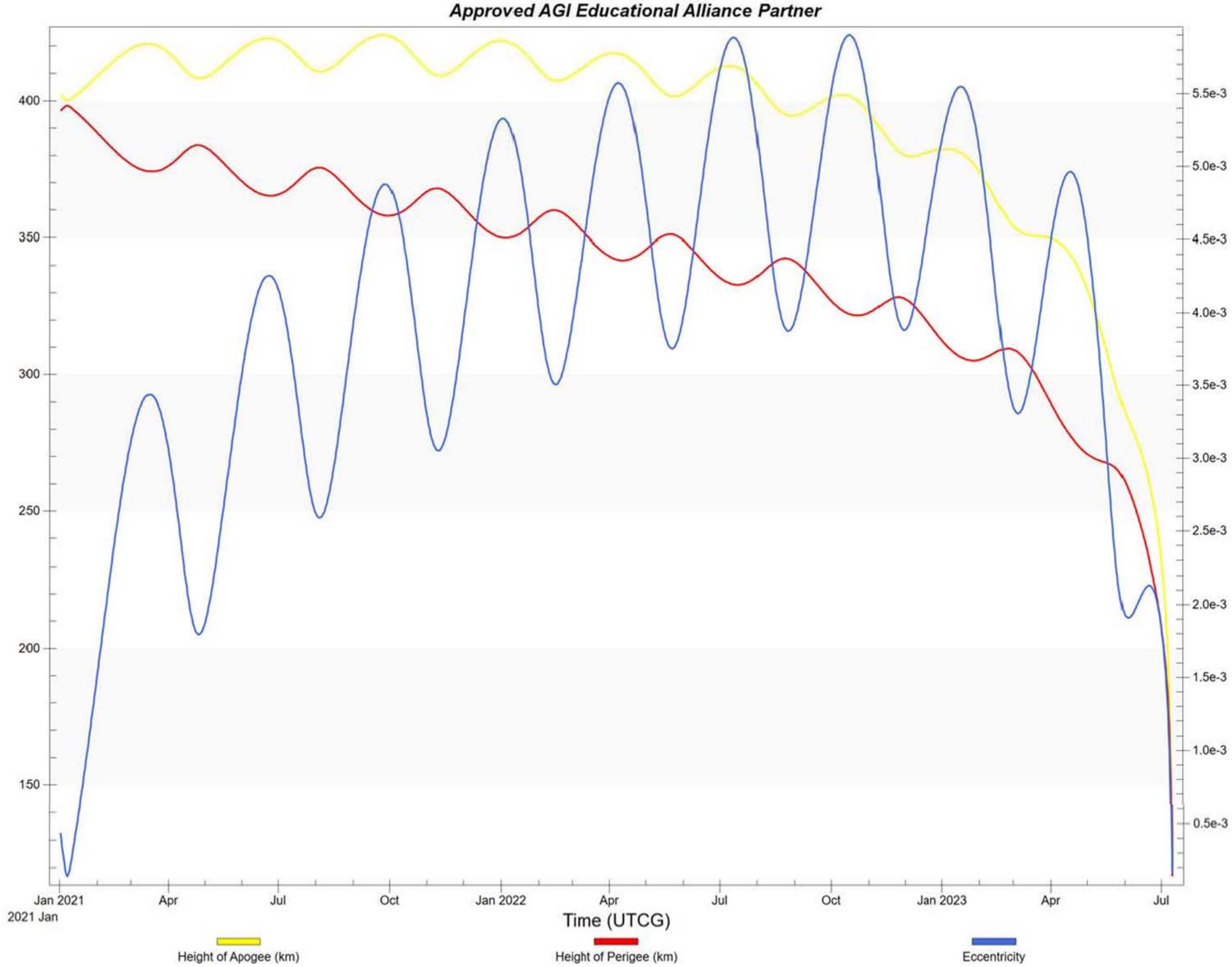

Figure 6: Best-Case Apogee and Perigee Altitude and Eccentricity [7]

Best-Case Scenario

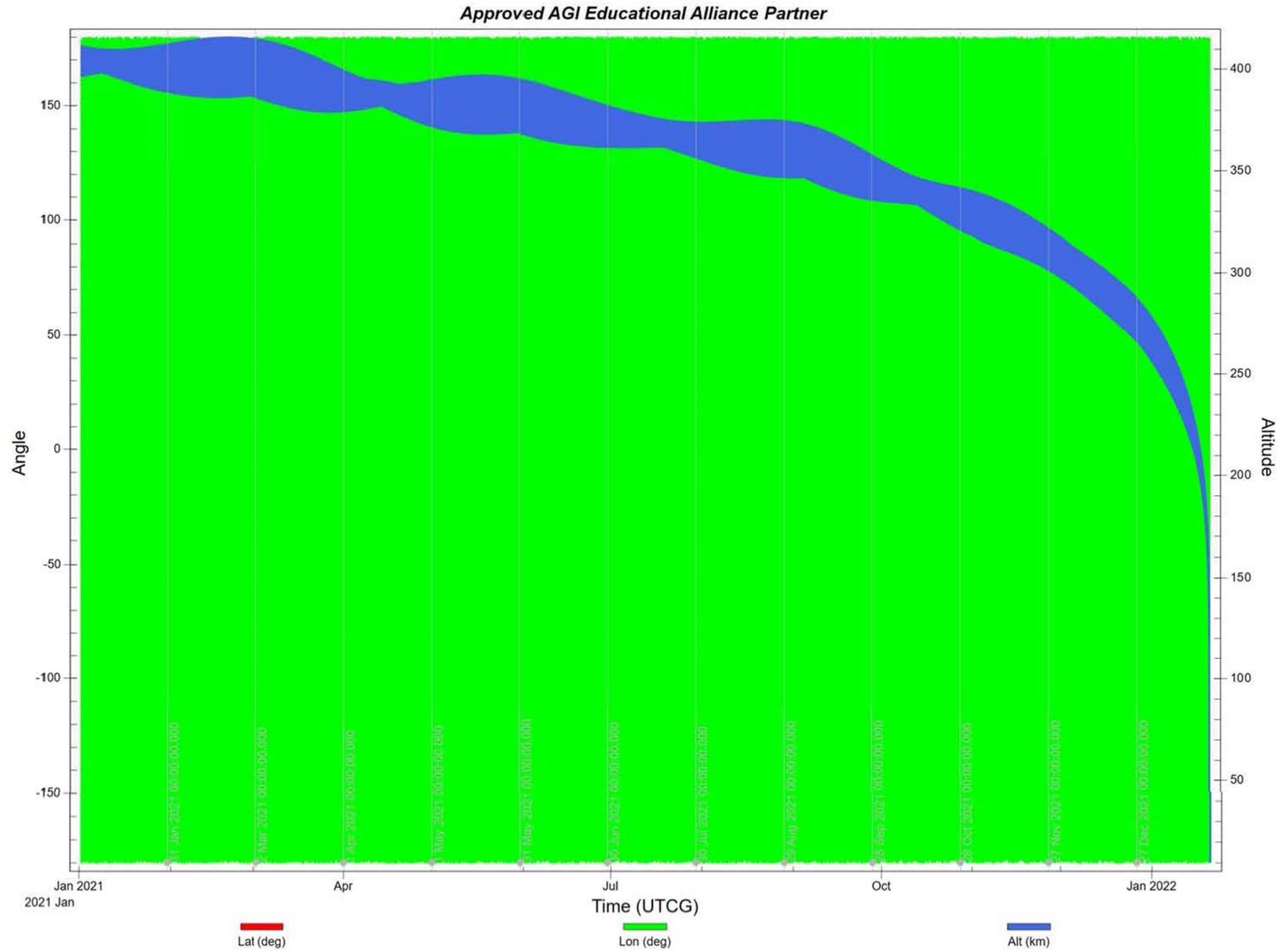

Figure 5: Best-Case Longitude, Latitude Altitude of CubeSat [7]

Best-Case Scenario

- Lifetime period with orbit deterioration effects:
  - 14,451 orbits
  - 2.5 years
  - January 1 2021 at 16:00:00.000UTC - July 10 2023 at 02:22:22:.286
  - Apogee altitude: 118.959209km at de-orbit
  - Perigee altitude: 116.88272km at de-orbit

Conclusions and Recommendations

Comparison

- Drag area and the area exposed to the sun decreased by 0.012862m^2 from the worst-case to the best-case scenario
- Modified upper atmospheric density model from the earlier 1977 Jacchia-Roberts model for the worst-case, to the NRLMSISE-00 as the latest empirical model for the best-case scenario
- Drag surface, area exposed to the sun, and atmospheric density models were the factors that greatest differ the lifetime computation

Comparison

- Differences in scenarios resulted in a significant difference of 5,479 orbits and 350 days
- CubeSat lifecycle range between 1.6 to 2.5 years
- Deorbit apogee altitude at 119.251142km for worst-case scenario and 117.52536km for best case-case scenario
- Deorbit perigee altitude at 118.959209km for worst-case scenario and 116.88272km for best case-case scenario

Challenges Encountered

- First satellite CubeSat project at Western, expected future changes for mass and size
- Large range of launch dates between 2020-2021
- Time variability in ISS deployment in LEO modifying orbital parameters
- Accuracy in selecting atmospheric density model, gravity force model, solar flux
- Uncertainty in drag coefficient, covariance amplitude oscillation, consider analysis

Recommendations

- Compare the accuracy of the computational lifetime models to orbit trajectory data received upon the CubeSat's launch to LEO
- Examine a further spectrum of atmospheric density models and potential drag area surfaces to investigate simulation sensitivity
- Provide analyzed data for next two years of mission preparation, operational cycle, and post-operational analysis in collaboration with interdisciplinary engineering teams

References

References

1. Canadian CubeSat Project Design Specification. [Accessed: 02-Jan-2019].

2. E. Mabrouk, "What are SmallSats and CubeSats?," *NASA*, 13-Mar-2015. [Online]. Available: https://www.nasa.gov/content/what-are-smallsats-and-cubesats. [Accessed: 02-Jan-2019].

3. ESA, "Technology CubeSats," *European Space Agency*. [Online]. Available: http://m.esa.int/Our_Activities/Space_Engineering_Technology/Technology_CubeSats. [Accessed: 02-Jan-2019].

4. D. A. Vallado and W. D. McClain, *Fundamentals of Astrodynamics and Applications,* 3rd ed. Hawthorne, CA: Microcosm Press, 2007.

5. M. F. Vess and S.R. Starin, "A Study On the Effects Of J2 Perturbations On A Drag-Free Control System for Spacecraft in Low Earth Orbit", *NASA Goddard Space Flight Center,* 2003.

6. [*NASA*. [Online]. Available: https://spaceflight.nasa.gov/realdata/sightings/SSapplications/Post/JavaSSOP/orbit/ISS/SVPOST.html. [Accessed: 02-Jan-2019].

7. *STK*. [Online]. Available: http://help.agi.com/stk/index.htm#stk/vehSat_orbitProp_msgp4.htm. [Accessed: 14-Jan-2019].

References

8. T. Prejean, “NanoRacks CubeSat Deployer (NRCSD) Interface Definition Document (IDD),” publication.

9. “ STK Engineering Tools,” *Agi*. [Online]. Available: https://www.agi.com/products/engineering-tools. [Accessed: 10-Mar-2019].

10. D. M. Prieto, B. P. Graziano, and P. C. Roberts, “Spacecraft drag modelling,” *Progress in Aerospace Sciences*, vol. 64, pp. 56–65, Sep. 2014.

11. J. T. Emmert and J. M. Picone, “Climatology of globally averaged thermospheric mass density,” *Journal of Geophysical Research: Space Physics*, vol. 115, no. A9, Sep. 2010.

12. V. U. Nwankwo, S. K. Chakrabarti, and R. S. Weigel, “Effects of plasma drag on low Earth orbiting satellites due to solar forcing induced perturbations and heating,” *Advances in Space Research*, vol. 56, no. 1, pp. 47–56, 2015.

13. G.-M. Chen, J. Xu, W. Wang, J. Lei, and A. G. Burns, “A comparison of the effects of CIR- and CME-induced geomagnetic activity on thermospheric densities and spacecraft orbits: Case studies,” *Journal of Geophysical Research: Space Physics*, vol. 117, no. A8, 2012.

14. K. Akins, L. Healy, S. Coffey, and M. Picone, “Effects of Solar Activity Level on Orbit Prediction Using MSIS and Jacchia Density Models,” *AIAA/AAS Astrodynamics Specialist Conference and Exhibit*, 2004.

References

15. J. Lafontaine and P. Hughes, "An analytic version of Jacchias 1977 model atmosphere," *Celestial Mechanics*, vol. 29, no. 1, pp. 3–26, 1983.

16. J. M. Picone, A. E. Hedin, D. P. Drob, and A. C. Aikin, "NRLMSISE-00 empirical model of the atmosphere: Statistical comparisons and scientific issues," *Journal of Geophysical Research: Space Physics*, vol. 107, no. A12, 2002.

17. D. L. Oltrogge and K. Leveque, "An Evaluation of CubeSat Orbital Decay", *25th Annual AIAA/USU Conference on Small Satellites*, 2011.

18. N. K. Pavlis, S. A. Holmes, S. C. Kenyon, and J. K. Factor, "The development and evaluation of the Earth Gravitational Model 2008 (EGM2008)," *Journal of Geophysical Research: Solid Earth*, vol. 117, no. B4, Apr. 2012.

19. "IERS Technical Note No. 36", *IERS*. [Online]. Available: https://www.agi.com/products/engineering-tools. [Accessed: 10-Mar-2019].

20. M. List, S. Bremer, B. Rievers, and H. Selig, "Modelling of Solar Radiation Pressure Effects: Parameter Analysis for the MICROSCOPE Mission," *International Journal of Aerospace Engineering*, vol. 2015, pp. 1–14, Oct. 2015.

Western
UNIVERSITY · CANADA